Chemical Engineering Journal 373 (2019) 1111–1119

Contents lists available at ScienceDirect

Chemical Engineering Journal

journal homepage: www.elsevier.com/locate/cej

Roles of Mg-Al layered double hydroxides and solution chemistry on P transport in soil

Xiaoqian Jiang[a,b], Miaoyue Zhang[c,d], Binggang Yan[e], Jiawei Hu[e], Jiayu Chen[a,b,f], Yuntao Guan[a,b,f,*]

[a] Graduate School at Shenzhen, Tsinghua University, PR China
[b] Guangdong Provincial Engineering Technology Research Center for Urban Water Cycle and Water Environment Safety, Graduate School at Shenzhen, Tsinghua University, PR China
[c] School of Environmental Science and Engineering, Sun Yat-sen University, Guangzhou, PR China
[d] Guangdong Provincial Key Laboratory of Environmental Pollution Control and Remediation Technology, Sun Yat-sen University, PR China
[e] School of Civil Engineering, Lanzhou University of Technology, Lanzhou, PR China
[f] State Environmental Protection Key Laboratory of Microorganism Application and Risk Control, School of Environment, Tsinghua University, Beijing 100084, PR China

HIGHLIGHTS

- Retention of P in the soil increased with the addition of LDHs and in the presence of Ca^{2+} in comparison to K^+.
- Both breakthrough curves and retention profiles for P were simulated by Hydrous 1D.
- A potential for Fe/Al oxides-facilitated transport of P under the change of soil solution chemistry.
- The dissolution and transport of LDHs could be impeded in the presence of high cation valence and IS.

GRAPHICAL ABSTRACT

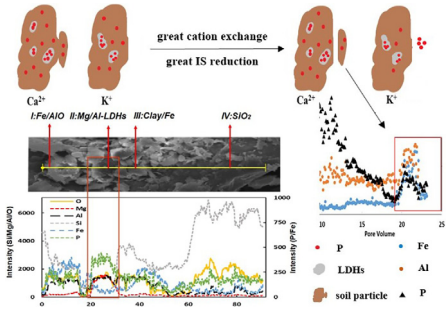

ARTICLE INFO

Keywords:
Phosphorus
Soil
Layered double hydroxides
Cation exchange
Breakthrough curves
Retention profiles

ABSTRACT

Mg-Al layered double hydroxides (LDHs) were synthesized and applied to soils to control phosphorus (P) loss. Saturated soil column experiments and numerical modeling were conducted to investigate the transport, retention, and release behavior of P in natural soil with and without mixing LDHs under various solution chemistries. Retention of P in the soil increased with the addition of 0.5% LDHs and in the presence of Ca^{2+} in comparison to K^+. The simulated results showed that irreversible retention of P is greater in the presence of Ca^{2+} than K^+ in soil without LDHs and in the presence of 0.5% LDHs in comparison to the absence. The increase of ionic strength (IS) for K^+ from 1 to 100 mM resulted in increased P retention in LDH-soil system due to more inner-sphere complexes and increased adhesive force. Near equilibrium retention on the reversible site occurred for all these experiments. The P was desorbed and the transport of dissolved P was improved with the reduction of IS in the presence of K^+. On the other side, larger ion exchange and reduction of IS in the presence of Ca^{2+} induced the release of Fe/Al oxides which brought transport of P absorbed on those minerals, suggesting the potential for Fe/Al oxides-facilitated transport of P under the change of soil solution chemistry. Additionally, the transport and stability of LDHs in soil column were also investigated. The dissolution and transport of LDHs could be impeded in presence of high cation valence and IS.

* Corresponding author at: Graduate School at Shenzhen, Tsinghua University, PR China.
E-mail address: guanyt@sz.tsinghua.edu.cn (Y. Guan).

https://doi.org/10.1016/j.cej.2019.05.083
Received 29 March 2019; Received in revised form 10 May 2019; Accepted 14 May 2019
Available online 15 May 2019
1385-8947/

1. Introduction

Phosphorus (P) is an essential macronutrient that is a limiting factor for biological productivity in terrestrial environments [1]. In agricultural soils, over-application of P to increase crop productivity has caused P losses to adjacent water systems and promoted diffuse pollution and eutrophication [2,3]. Reducing soil P leaching and improving P long-term availability have therefore been hot topics for P nutrient management in soil.

Layered double hydroxides (LDHs) have a very high P sorption capacity (e.g. $\sim$2.25 mmol L^{-1}) [4]. Recent research studies have investigated LDHs as promising phosphate adsorbents in waste streams due to their high charge density sheets, large interlayer areas, and high anion exchange capacity [4–6]. Runoff losses of P have also been shown to be significantly reduced when using P-LDHs fertilizer in soils [7]. However, little research attention has focused on the direct application of LDHs in soil to decrease P leaching and dissemination in the environment. This study is one of the first to investigate the role of LDHs for the control of soil P loss.

LDHs loaded with P can serve as controlled released fertilizers that can maintain plant availability to P over longer periods than conventional fertilizers [8–11]. In particular, the availability of P on LDHs was higher than that of traditional fertilizers in both acid and calcareous soils [8,12]. These results imply that adsorbed P on LDHs may be slowly released to the plants. Therefore, the addition of LDHs to soils is beneficial for both soil P loss control and increased availability to plants.

The adsorption behavior of anions on LDHs in aqueous and packed-bed columns has been investigated under various physical and chemical conditions including solution pH [1,4,5], soil types [8], and particle sizes [5]. The retention of engineered nanoparticles (ENPs) in soils can be enhanced at a higher ionic strength (IS) [13–15] and by changing monovalent to divalent cations [16–19] due to an increase in the adhesive force. Accordingly, the attachment of LDHs that are associated with P is expected to be influenced by the IS, cation valence, and cation exchange. However, little research attention has focused on P adsorption and LDH attachment behavior under different soil solution chemistry conditions such as ion type and IS.

The objective of this study is to better understand roles of LDHs, solution IS, and cation type on the transport, retention, and release behaviors of P in natural soil. Breakthrough curves and retention profiles for P and LDHs were investigated in column experiments, and a numerical model was employed to simulate the fate of P. Additional experiments were conducted to determine the release of P and LDHs with perturbations in solution chemistry (i.e. IS reductions and cation exchange). This knowledge can be useful for environmental applications and risk management for surface water eutrophication and soil intensive fertilization.

2. Materials and methods

2.1. Soil and LDHs

Soil samples were collected from the upper 20 cm of an agriculture field site in Shuyang, China, air dried and sieved to < 2 mm. The soil contained 6.4% clay, 52% silt, and 41.6% sand according to the method by Bouyoucos [20]. It had a total organic carbon content of 0.14 ± 0.01%, and a neutral pH value of 7.08 ± 0.04. Mg/Al-LDHs were prepared by the co-precipitation method [4]. In brief, a 600 mL mixture of $MgCl_2$ and $AlCl_3$ aqueous solution with $[Mg^{2+}]/[Al^{3+}]$ ratio = 2 and $[Mg^{2+}] + [Al^{3+}] = 1$ M was added dropwise ($\sim$2.5 mL min^{-1}) into a flask containing 600 mL of a 1 M NaCl solution. The addition was performed under vigorous stirring at pH $\sim$ 8.5–9 and fixed with a 2 M NaOH solution. The synthesis was performed under nitrogen bubbling to minimize carbonate intercalation. Once the addition of reactants was finished, the mixture was maintained under stirring, nitrogen bubbling and pH control for 2 h. The solid precipitate of LDHs was then separated by centrifugation, washed several times with Milli-Q water and finally dried in air at 60 °C. The collected LDHs was ground and sieved using a mesh screen (No. 100). The Mg and Al concentrations of LDHs was determined by inductively coupled plasma optical emission spectrometer (ICP-OES) after dissolving in 3.6 M H_2SO_4. The powder X-ray diffraction (XRD) pattern and scanning electron microscope-energy dispersive spectrometer (SEM-EDS) images were obtained to characterize LDHs. Additionally, the zeta potentials of LDHs and soil in KCl and $CaCl_2$ solutions at different IS (1, 5, 10, 20, 50, 100 mM) were determined using a Zetasizer Nano Apparatus (Zetasizer Nano ZS90, RI: 1.54, Absorption: 0.05).

2.2. Transport and retention experiments

Various electrolyte solutions were prepared in Milli-Q water using different cation types (i.e., 1 mM K^+ and Ca^{2+}, molar concentration 1 mmol L^{-1} KCl and 0.33 mmol L^{-1} $CaCl_2$) and IS (1, 10, 20, and 100 mM KCl). The P solution was prepared by adding KH_2PO_4 (0.75 g P L^{-1}) to Milli-Q water for transport experiments in the presence of K^+. It is worth noting that the P solution in Milli-Q water contains 24 mM K^+ and we did not prepare it in the different IS K^+ solution to avoid two variational IS in a transport experiment. The P transport experiments were conducted in packed columns with and without the addition of 0.5% LDHs to the soil. Soils were mixed with 0.5% of LDHs by shaking over 1 h vertically at 280 rpm before column packing. The porosity of the packed column was approximately 0.5. The approach for column experiments has been previously described by Zhang et al. [19]. In brief, steady-state flow from the column bottom to the top was achieved using a peristaltic pump. The packed column was equilibrated before initiating the transport experiment by slowly injecting (Darcy velocity of 0.16 cm min^{-1}) approximately 20–25 pore volumes of a selected background electrolyte solution. The transport experiment for P consisted of injecting a 1.8 pore volume pulse of P solution, followed by continued eluting with the same background electrolyte solution for another 4.1 pore volumes at a constant Darcy velocity of 0.32 cm min^{-1}. The effluent concentrations of P were determined using the ICP-OES. After recovery of the breakthrough curve (BTC), the P retention profile (RP) was determined by excavating soil samples from the column in 1 cm increments. The collected soil in each sample was extracted with $\sim$50 mL of Milli-Q water, followed with $\sim$30 mL of 3.6 M H_2SO_4 then with $\sim$50 mL of Milli-Q water to determine the P concentration in the soil. Preliminary experiments demonstrated that LDHs could be dissolved with 3.6 M H_2SO_4 and the recovery of added P concentration was 99.8% with this extraction method (shown in Supporting information). Soil samples from the P transport experiment in presence of 1 mM K^+ and 0.5% LDHs were collected for measurement with the SEM-EDS. A summary of the experimental conditions is provided in Table 1. All the experiments were replicated and exhibited similar results.

A control experiment in the presence of 1 mM K^+, but without P injection, was operated in a similar manner to determine the background value of P in the soil. The effluent concentrations of P for this control experiment were extremely low and negligible.

2.3. Release experiments

The release behavior of retained P in the LDHs-soil with IS reduction and cation exchange was investigated to assess its stability and the distribution of LDHs. The P transport experiment in the presence of 100 mM K^+ was conducted as discussed in the section 2.2 and subsequently the background solution was changed to Milli-Q water for another 5.9 PVs. For release experiments in the presence of Ca^{2+}, the initial transport experiment (Step 1) was conducted using KH_2PO_4 (0.75 g P L^{-1}) in 1 mM (Ex. I) and 10 mM (Ex. II) Ca^{2+} for soil with 0.5% LDHs, as well as 1 mM Ca^{2+} for soil without LDHs (Ex. III). The release experiments were then initiated by changing the elution

Table 1
Experimental conditions, hydraulic parameters and mass balance information for all column experiments.

	IS (mM)	Cation	Solution pH	LDHs (%)	C_0 (g L^{-1})	Darcy (cm min^{-1})	φ	M_{eff} (%)	M_{soil} (%)	M_{total} (%)
Fig. 2	1	K	5.76 ± 0.08	0	0.76	0.31	0.55	84.1	15.7	99.8
	1	K	5.76 ± 0.08	0.5	0.76	0.32	0.51	54.4	43.9	98.3
	1	Ca	5.32 ± 0.01	0	0.76	0.32	0.5	68.5	27.9	96.4
	1	Ca	5.32 ± 0.01	0.5	0.75	0.30	0.5	48.9	47.8	96.7
Fig. 3	1	K	5.76 ± 0.08	0.5	0.76	0.32	0.51	54.4	43.9	98.3
	10	K	5.38 ± 0.04	0.5	0.76	0.31	0.5	48.3	41.2	89.5
	20	K	5.16 ± 0.02	0.5	0.74	0.35	0.5	48	45.6	93.6
	100	K	5.01 ± 0.06	0.5	0.71	0.31	0.5	44.3	54.8	99.1
Fig. 5	100–0	K	5.01 ± 0.06	0.5	0.72	0.31	0.48	53.7	45.3	99.0
Ex. I	1	Ca-K	5.32 ± 0.01	0.5	0.77	0.31	0.51	58.0	39.5	97.5
Ex. II	10	Ca-K	4.87 ± 0.03	0.5	0.76	0.35	0.5	55.9	31	86.9
Ex. III	1	Ca-K	5.32 ± 0.01	0	0.76	0.32	0.5	85.1	17.3	102.4

Fig. 2: cation type and LDHs effect; Fig. 3: ionic strength effect; Fig. 5: release of P by ionic strength reduction and cation exchange; C_0, P input concentration; IS, ionic strength; φ, porosity; M_{eff}, M_{soil}, and M_{total} are mass percentages of injected phosphate recovered from effluent, soil, and total, respectively.

solution chemistry in the following sequence: Milli-Q water for 5.9 PVs (Step 2); KCl at the same IS as in step 1 for 1.8 PVs (Step 3); Milli-Q water for 4.1 PVs (Step 4); 100 mM KCl for 1.8 PVs (Step 5); and Milli-Q water for 4.1 PVs (Step 6). The concentrations of P in the effluent and soil were measured in the same manner as in transport experiments. Cation exchange and soil/LDHs were quantified by measuring concentrations of K, Ca, Fe, Al, and Mg using the ICP-OES. In order to investigate the impact of cation exchange and IS reduction on LDHs transport in the soil column system, the Mg concentration in excavated soil samples was determined following the release experiment using same process as in Section 2.2. The Mg concentration distribution in the soil column without LDHs was used to determine its background level. A Mg concentration above the background value was considered as an indication of the LDHs concentration. Additionally, released colloids in the effluent of Step 6 of Ex. I were characterized by SEM-EDS.

2.4. Numerical modelling

The one-dimensional transport of P in soil columns with and without LDHs was simulated using the HYDRUS 1D code [21]. Transport was described using the advection-dispersion equation with two kinetic retention sites as [22,23]:

$$\frac{\partial \theta c}{\partial t} + \rho_b \frac{\partial (S_1)}{\partial t} + \rho_b \frac{\partial (S_2)}{\partial t} = \frac{\partial}{\partial x}\left(\theta D \frac{\partial c}{\partial x}\right) - \frac{\partial qc}{\partial x} \quad (1)$$

where θ is the volumetric water content, c is the phosphate concentration in the aqueous phase [M L^{-3}], where L and M denote units of length and mass of P, respectively, ρ_b is the bulk density of the soil matrix [M_s L^{-3}, where M_s denotes the soil mass], t is the time [T denotes units of time], x is the vertical spatial coordinate [L], D is the hydrodynamic dispersion coefficient [L^2 T^{-1}], q is the Darcy velocity [L T^{-1}], and S_1 [M M_s^{-1}] and S_2 [M M_s^{-1}] are the phosphate concentrations associated with retention sites 1 and 2, respectively.

The two kinetic sites were needed to accurately describe the retention of phosphate on the soil with/without LDHs [24]. The first kinetic site (Eq. (2)) assumes irreversible retention and Langmuirian blocking, whereas the second kinetic site (Eq. (3)) considers reversible retention as:

$$\rho_b \frac{\partial (S_1)}{\partial t} = \theta k_1 \psi c \quad (2)$$

$$\rho_b \frac{\partial (S_2)}{\partial t} = \theta k_2 c - \rho_b k_{2d} S_2 \quad (3)$$

where k_1 [T^{-1}] and k_2 [T^{-1}] are first-order retention rate coefficients on site 1 and 2, respectively, and k_{2d} [T^{-1}] is the release rate from site 2. The Langmuirian blocking function, ψ [–], decreases k_1 in a linear manner with increasing S_1 as available retention sites fill and is given by:

$$\psi = \frac{S_1}{S_{max1}} \quad (4)$$

where S_{max1} [M M_s^{-1}] is the maximum potential concentration of phosphate on site 1.

BTCs and RPs from the P transport experiments were analyzed using the HYDRUS-1D code to fit the phosphate transport parameters (k_1, S_{max1}, k_2, and k_{2d}) using a nonlinear least square optimization routine based on the Levenberg-Marquardt algorithm [25].

3. Results and discussion

3.1. Characterization of LDHs and zeta potentials

The ICP-OES results show that the Mg/Al mole ratio is 1.9 for Mg-Al-LDHs. The XRD pattern of Mg/Al-LDHs is given in Fig. S1a. The result shows the typical XRD pattern of a pure hydrotalcite, which is consistent with other findings in the literatures [4,9,26,27]. Fig. S1b displays the SEM image of the synthesized Mg/Al-LDHs. These uniform and regular LDHs platelets are similar to those shown by Berber et al. [25], and confirm the good crystallinity in XRD results.

Fig. 1 presents plots of measured zeta potentials (ξ) for LDHs, soil, and LDHs-soil as a function of IS and cation valence (K^+ and Ca^{2+}). The

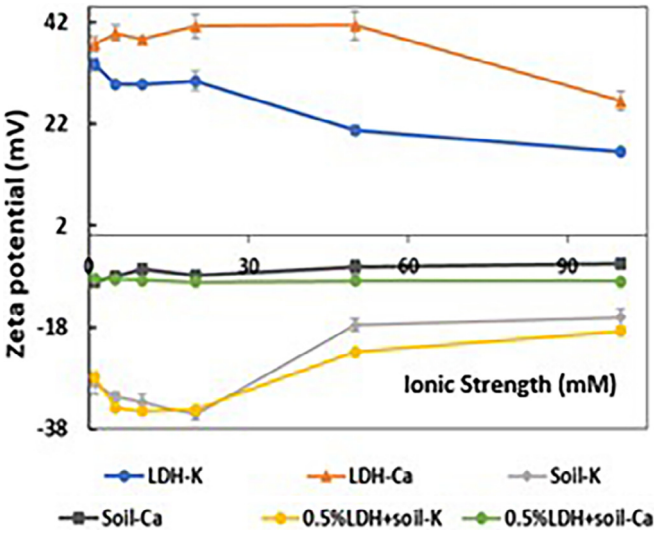

Fig. 1. Zeta potential values of LDHs, soil, and LDHs-soil (i.e. 0.5% LDHs) as a function of the solution (KCl and $CaCl_2$) ionic strength (IS = 1, 5, 10, 20, 50, and 100 mM, respectively).

LDHs and soil exhibited positive and negative charges, respectively, for all selected solution chemistries, which indicates that there are attractive electrostatic interactions between LDHs and soil. These results suggest that the addition of LDHs could increase the sorption of phosphate by increasing the number of positively charged sites in the soil. However, the addition of 0.5% LDHs in the soil did not significantly change the net value of the ξ (Fig. 1). Additionally, a change in the IS using Ca^{2+} had little influence on the charge of the soil with and without 0.5% LDHs. For LDHs, increasing the IS from 50 to 100 mM using Ca^{2+} ions decreased the value of ξ. The charge of soil, LDHs, and LDHs-soil was more sensitive to change in IS using K^+ and the absolute value of charge significantly decreased when the IS increased above 20 mM K^+. These changes of ξ with IS suggested that altering IS of K^+ will have a greater influence on phosphate sorption and transport than changing IS of Ca^{2+}. Furthermore, Ca^{2+} and K^+ have a significantly different influence on charge of all LDHs, soil, and LDHs-soil, which indicates that the cation valence may have an effect on phosphate absorbed in LDHs-soil. Therefore, in the following transport experiment, we compared the influence of IS in the presence of K^+ and the influence of cation valence on P transport and retention in the column.

3.2. Transport and retention of P

The effect of cation valence and LDHs on the transport and retention of P in soil was presented in Fig. 2. The background solution chemistry for these experiments was IS = 1 mM in the presence of monovalent K^+ or divalent Ca^{2+} cation. The BTCs (Fig. 2a) are plotted as the normalized effluent concentration (C/C_0) of phosphate versus pore volumes and the RPs (Fig. 2b) are plotted as normalized solid phase concentration of injected phosphate (S/C_0) as a function of distance from the column inlet. Table 1 summarizes the experiment conditions, hydraulic parameters, and mass balance of information for all experiments. The total mass balance (M_{total}) of all column experiments for injected phosphate in Fig. 2 was always greater than 96% (Table 1), and this indicates that our experimental procedures provided good P recovery.

The mass percentage of phosphate recovered from the effluent (M_{eff}) strongly decreased by 19.6–29.7% for both cation types when 0.5% LDHs was added to the soil, resulting in a corresponding increase in the solid phase mass percentage (M_{soil}) in Table 1. These trends are attributable to an increase of adsorption sites of phosphate. The phosphate adsorption on LDHs occurs via three different adsorption modes: electrostatic attraction, anion exchange, and surface complexation [4]. The positive charge of LDHs creates a favorable chemistry for binding negatively charged phosphate and adsorption of phosphate takes place by anion exchange with interlayer chloride ions. Additionally, phosphorus acts as a ligand that binds directly to Al^{3+} or Mg^{2+} ions at the surface [4]. The value of M_{soil} also increased by 3.9–12.2% in the presence of Ca^{2+} than M_{soil} in the presence of K^+ in both soil and LHDs-soil. Several factors can contribute to increased phosphate retention in the presence of Ca^{2+} than K^+. For example, increasing Ca^{2+} concentration could facilitate the formation of Ca-bound P as metastable minerals in the column [28,29]. Also Ca^{2+} can produce a stronger adhesive force for LDHs-soil by localized cation bridging [16,19], and/or neutralization or reversal of surface charge [30] which reduces the net magnitude of ξ (Fig. 1) and thus increases the adsorption of phosphate. In addition, phosphate desorption is reported to be greater in the presence of K^+ than Ca^{2+} [31].

Fig. 2a shows a smaller increase in the BTC in the presence of Ca^{2+} than for K^+. In general, the breakthrough curves indicate that the effect of Ca^{2+} is more apparent in the absence than the presence of LDHs. Similar tailing behavior occurs in all BTCs and plays a relatively small role in comparison to irreversible retention. The BTCs and RPs for phosphate were well described using the transport model with two kinetic retention sites ($R^2 > 0.94$). Table 2 presents fitted retention model parameters and the R^2 value for the goodness of fit in experiments. The RPs profiles mainly reflect the amount of irreversible retention (site 1). As discussed above, irreversible retention (S_{max1}) was greater in the presence of 0.5% LDHs in comparison to the absence (Table 2). For the irreversible site 1, the value of k_1 and S_{max1} are much larger in the presence of Ca^{2+} than for K^+ for soil without LDHs. The presence of LDHs increased both k_1 and S_{max1} in the presence of K^+, whereas it only increased S_{max1} in the presence of Ca^{2+} (Table 2). The tailing portion of the BTCs reflects the reversible retention site 2. Values k_{2d} were larger than k_2 for all the experiments and this reflected a rapid release process that exhibited near equilibrium transport behavior [32].

Fig. 3 presents observed and simulated BTCs and RPs for phosphate in soil with 0.5% LDHs when the IS = 1, 10, 20, and 100 mM KCl. All the BTCs for phosphate exhibited increasing breakthrough concentrations over time due to blocking; i.e., filling of a limited number of retention sites with continued phosphate injection. The effect of IS has normally been correlated with the type of outer-sphere and inner-sphere surface complexes [33,34]. Adsorbed P forming outer-sphere complexes via electrostatic interaction could compete with the supporting electrolyte ion (i.e. Cl^-) for adsorption on surface sites. In this case, adsorption of phosphate decreases with increasing IS [35]. On the other hand, no or less competition occurs when PO_4^{3-} forms inner-sphere complexes, which are coordinated to a surface group via ligand exchange directly [35]. Moreover, increasing IS modified the electrical potential at the interface and decrease the electrostatic repulsion between the charged surface and ion, thus favoring adsorption process which have been implicated in many cases with inner-sphere

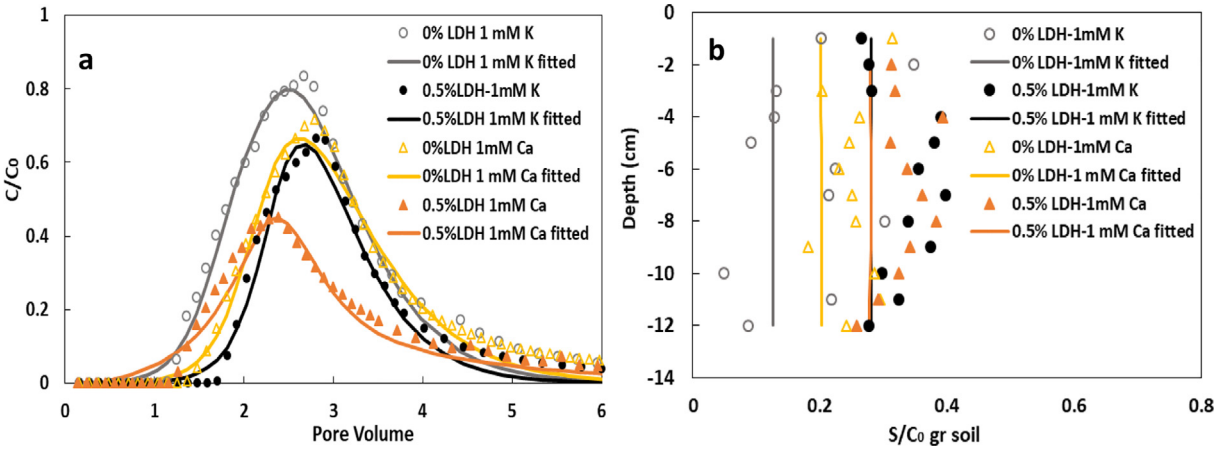

Fig. 2. Effect of cation type and LDHs on the transport and retention of P in soil: observed and fitted breakthrough curves (a) and retention profiles (b) of P under 1 mM K^+ and Ca^{2+} with and without 0.5% LDHs. C_0: P input concentration. S: normalized solid phase concentration of injected P after transport experiment.

Table 2
Fitted model parameters.

	IS (mM)	Cation	LDHs (%)	k_1 (T^{-1})	S_{max1} ($M M_s^{-1}$)	k_2 (T^{-1})	k_{2d} (T^{-1})	R^2
Fig. 2	1	K	0	3.52E−01	1.25E−01	1.56E−01	4.61E−01	0.962
	1	K	0.5	6.92E−01	2.80E−01	1.58E−01	6.02E−01	0.966
	1	Ca	0	5.48E−01	2.02E−01	1.45E−01	3.07E−01	0.974
	1	Ca	0.5	2.28E−01	2.73E−01	1.94E−02	4.21E−02	0.947
Fig. 3	1	K	0.5	6.92E−01	2.80E−01	1.58E−01	6.02E−01	0.966
	10	K	0.5	7.83E−01	3.03E−01	1.27E−01	3.13E−01	0.966
	20	K	0.5	6.91E−01	3.19E−01	1.07E−01	2.29E−01	0.962
	100	K	0.5	4.82E−01	2.67E−01	9.40E−03	1.74E−05	0.963

Fig. 2: cation type and LDHs effect; Fig. 3: ionic strength effect; IS: ionic strength; R^2 reflects the correlation of observed and fitted data; k_1 and k_2, the first-order retention rate coefficients on site 1 and 2, respectively; k_{2d}, the first-order release rate coefficient from site 2; S_{max1}, normalized maximum solid phase concentration of deposited phosphate on site 1.

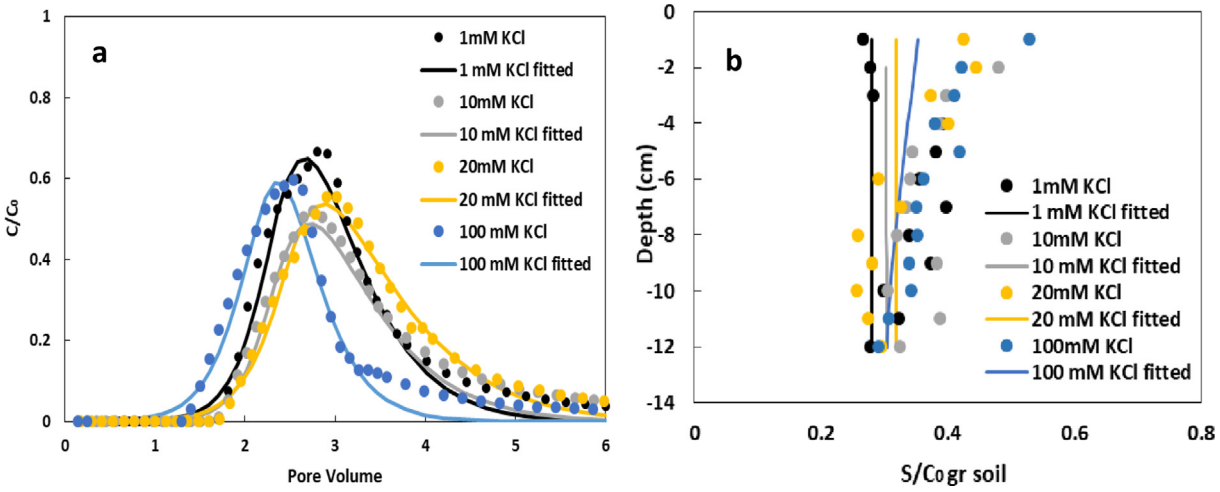

Fig. 3. Effect of ionic strength on the transport and retention of P in soil: observed and fitted breakthrough curves (a) and retention profiles (b) of P under 1, 10, 20, and 100 mM KCl, respectively.

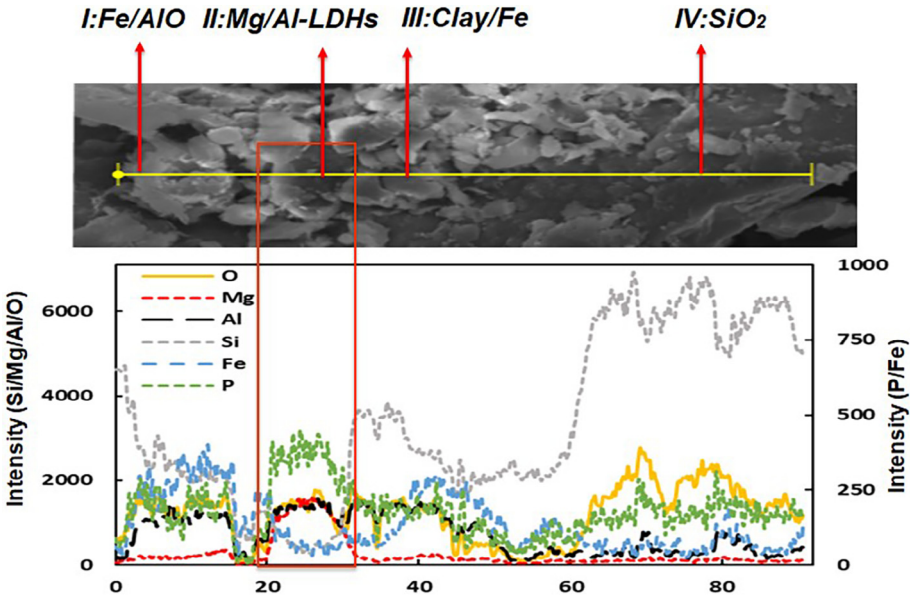

Fig. 4. Scan electron microscope (SEM) and corresponding energy dispersive spectrometer (EDS) for line scan (i.e. the part of yellow line in SEM image) for LDHs added soil sample after P transport with 1 mM KCl as background solution. (For interpretation of the references to colour in this figure legend, the reader is referred to the web version of this article.)

complexation [33–36].

In our case, the M_{soil} seems increasing slightly with IS although it is not obvious for IS ≤ 10 mM (Table 1), probably due to increasing phosphate adsorption by more inner-sphere complexes and increased adhesive force. For the reversible site 2, the k_2 and k_{2d} for IS = 10 and 20 mM decreased in comparison with IS = 1 mM (Table 2). For the irreversible site 1, the values of S_{max1} increase slightly when IS increased from 0 to 20 mM (Table 2). These results reflected a relatively higher contribution of irreversible retention in comparison with reversible retention for the amount of retained phosphate in LDHs-soil. For the IS = 100 mM, the values of k_1, S_{max1}, k_2, and k_{2d} are the smallest in spite of the largest amount of phosphate retained in LDHs-soil. There

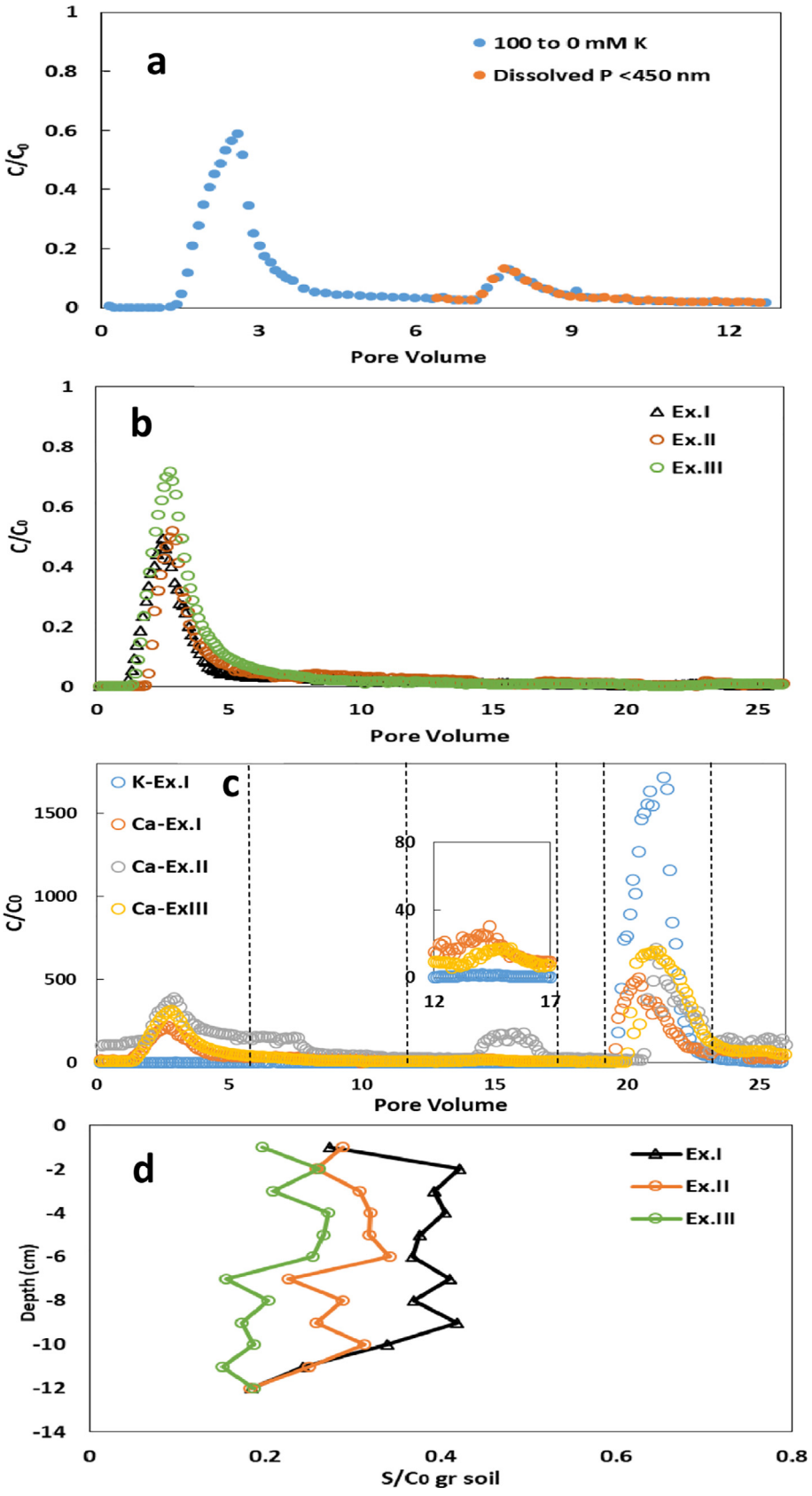

Fig. 5. Breakthrough and release behavior of P (a) for the release experiment with IS reducing from 100 to 0 mM in the presence of K^+, and P (b), K, and Ca (c) as well as retention profiles of P in soil (d) for experiments I, II, and III, respectively.

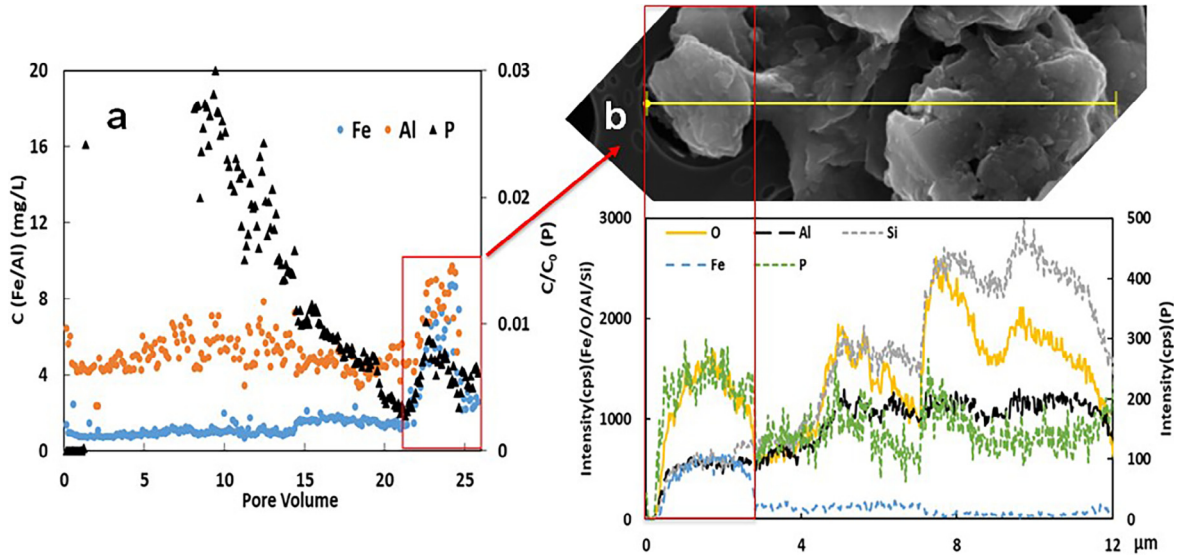

Fig. 6. Release behavior of P, Fe, and Al (left) and scan electron microscope (SEM) and corresponding energy dispersive spectrometer (EDS) for line scan (i.e. the part of yellow line) for the released particle during step 6 of experiment I. (For interpretation of the references to colour in this figure legend, the reader is referred to the web version of this article.)

is a complicated situation for the experiment in the presence of IS = 100 mM K^+: the injection of phosphate solution with ~24 mM K^+ brought a relatively decreasing IS and the following injection of background solution brought increasing IS. In the study of Jensen et al. [31], the transport of dissolved inorganic P through an intact water-saturated column was improved with decrease of IS of the infiltration solution. It suggested that desorption and release of phosphate from soil-LDH particles increase with the decreasing of IS. Correspondingly, the earlier elution of phosphate for IS = 100 mM than smaller IS may be due to desorption and release of phosphate during the injection of phosphate solution. The fitted results for 100 mM K^+ may reflect the results for decreased IS during phosphate injection but could not simulate the whole complicated transport experiment accurately.

Fig. 4 presents the line scan result of SEM and corresponding EDS for 0.5% LDHs soil sample after completion of a P transport experiment at the presence of 1 mM K^+. We found Fe/Al oxides, Mg/Al-LDHs, Fe bearing clay, and SiO_2 minerals in the sample according to the line scan of elemental composition measured by EDS. The intensity of P is the highest with Mg/Al-LDHs mineral and is also relatively high with Fe/Al oxides compared to other minerals (Fig. 4). Many researchers have already reported that P was dominantly associated with amorphous Fe and Al oxides fractions in various soil types in the USA and Europe [34,37,38]. Our SEM-EDS result confirmed that more P was adsorbed to Mg/Al-LDHs than Fe/Al oxides. This information clearly shows that Mg/Al-LDHs are effective adsorbents for phosphate in soil.

3.3. The roles of IS reduction, cation valance, and exchange on release of phosphate

Fig. 5a presents the BTC for the phosphate transport experiment in the presence of 100 mM K^+ for the first 5.9 PVs and then the background solution of 100 mM K^+ was changed to Milli-Q water (i.e. 0 mM K^+) for another 5.9 PVs. A certain amounts of phosphate (12.8%) was eluted when IS changed from 100 to 0 mM (Fig. 5a). Then the effluents were filtered with 450 nm membrane (i.e. dissolved P) and the amounts of dissolved P in the effluents were similar with the eluted total P. As discussed before, desorption and release of phosphate from soil-LDHs particles increase with the decreasing of IS in the presence of K^+.

For the experiment I, II, and III, all the transports of phosphate occur mainly in the first step (i.e. P transport experiment) where IS of Ca (1 mM or 10 mM) are smaller than those of K (~24 mM, the injection of KH_2PO_4, Fig. 5b). The $CaCl_2$ has been injected around 20–25 pore volumes as background solution before the transport experiment. However, Ca was eluted instead of K which indicated that ion exchange has occurred in the first step for all the experiments. Little amounts of released phosphate have been reported when transient solution chemistry reduce the adhesive force (i.e. the injection of Milli-Q water in the step 2). Moreover, in step 3 and 4, increasing cation exchange in experiment II (i.e. the release of more Ca by injecting K) and following reducing of IS (i.e. the injection of Milli-Q water in step 4) could not enhance the release of phosphate compared to experiment I. All those results indicated that the adsorption of phosphate on soil and LDHs particles in the presence of Ca^{2+} is strong enough and cation exchange as well as change of IS have little influence on the release and desorption of P retained in soil. Additionally, when IS of K increased significantly to 100 mM (i.e. Step 5) and then reduced to 0 mM (i.e. injection of Milli-Q water in step 6), substantial release of Ca^{2+} was produced as a result of cation exchange. Consequently, a small amounts of particles were released during following IS reduction from 100 to 0 mM (i.e. step 6). The enlarged BTC of experiment I (Fig. 6a) indicated that a small peak containing P, Fe, and Al occurred during step 6, which suggested that phosphate was released with Fe/Al oxides minerals. This result was also confirmed with the line scan result of SEM-EDS for released particles (Fig. 6b). These released particles contained Fe oxides, SiO_2, and clay minerals according to the EDS results of line scan of particles (Fig. 6b). We found that P was enriched with minerals dominated by Fe and O, i.e. Fe oxides minerals (Fig. 6b). Thus we concluded that the release of P in the presence of Ca^{2+} is possible in a certain situation: the ion exchange and reduction of IS need to be large enough to release small-sized soil particles and P adsorbed on those particles could be released correspondingly. The colloid-facilitated transport of multi-walled carbon nanotubes (MWCNTs) and silver nanoparticles were also reported and the release behavior of those, Fe, and Al closely follow each other with cation exchange and IS reduction [18,19]. All of these observations support the potential for Fe/Al oxides-facilitated transport of P during release experiments. Also, compared to P transport experiments at the presence of 1 mM Ca^{2+} as shown in Fig. 2, the transported amounts of P in Ex. I and III were higher after release experiments which is consistent with the discussion above (Table 1). Fig. 5d presents the RPs for P following completion of the release experiments. Similar to other RPs for Ca^{2+} as background solution (Fig. 2), the P distribution has no significant difference with column depth.

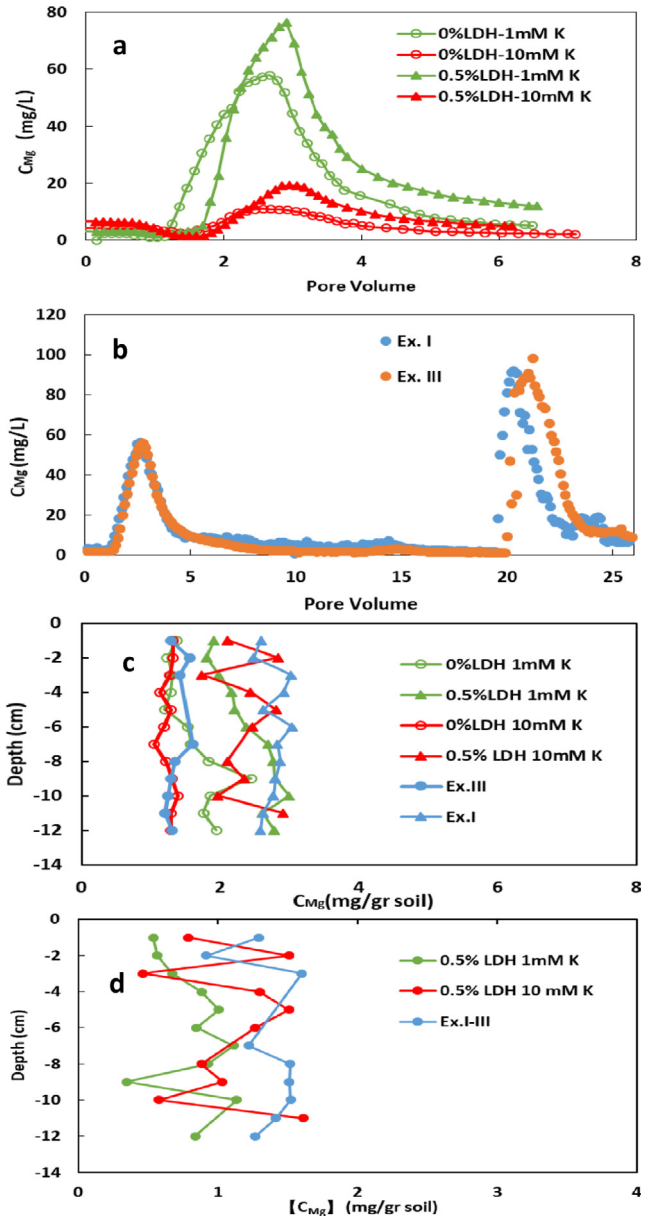

Fig. 7. The transport (a,b) and retention (c) of Mg concentrations for column experiments with different ion strength of KCl (i.e. 1 and 10 mM) and amounts of LDHs (i.e. 0% and 0.5%) as well as for experiment I and III. [C_{Mg}] (d) indicates the concentration of retained LDHs in soil.

3.4. Stability and distribution of Mg/Al-LDHs

To further confirm the stability and distribution of Mg/Al-LDHs in soil column, Fig. 7 presents the BTCs and RPs for Mg concentrations with and without mixing 0.5% LDHs in soil column. For IS = 1 and 10 mM K^+, the addition of LDHs caused higher BTCs for Mg than that without LDHs (Fig. 7a). The Al concentrations in BTCs for all soil columns with and without addition of Mg/Al LDHs are extremely low (data not shown), which indicated that the increasing Mg in BTCs is probably from the dissolution of Mg/Al-LDHs instead of the release of Mg/Al-LDHs particles. The partial dissolution of LDHs has been found in many researches and the increase of solubility of LDHs after phosphate adsorption has also been reported [39–41]. The solubility of LDHs in soil is probably due to the complexity of soil environment and can be highly affected by soil reactions such as complexation and precipitation of aluminum with organic and inorganic anions [42]. Furthermore, the phosphate adsorption with decreasing degree of crystallinity of LDHs can also increase the solubility of LDHs in soil [42]. Additionally, pH and particle size are also be factors affecting on LDHs solubility in solution: high pH and large particles could impede high dissolution [4,43–45]. On the other side, Fig. 7 presents the influence of IS (Fig. 7a) and cation types (Fig. 7a and b) on the dissolution of LDHs. The difference of transported Mg concentrations with and without LDHs (i.e. the amount of dissolved LDHs) decreased with higher IS (Fig. 7a). Additionally, the difference could be negligible for Ca^{2+} as background solution: the BTCs of Mg during P transport are similar in soil columns with and without mixing 0.5% LDHs (Fig. 7b, Step 1). Moreover, even the following ion exchange and change of IS could not cause more transport of Mg from LDHs and the difference of transported Mg concentrations was negligible between the whole Ex. I and III (Fig. 7b). On the other word, high cation valence impeded the transport of Mg from LDHs even under the change of solution chemistry. It should be mentioned that the solubility of LDHs increased with increasing IS in solution according to the research from Halajnia et al. [42]. Increasing interactions between solute and solvent ions in higher IS cause more dissolution of solvent because of the activity coefficients to maintain a constant solubility product at equilibrium [46]. Our results suggested that higher cation valence and IS could impede the transport of Mg dissolved from LDHs and the dissolution of LDHs may be different between solution and soil systems under conditions related to IS and cation valence. This could be explained by increasing bridging complexation and interaction between soil grains and LDHs particles in the presence of Ca^{2+} or higher IS and thus impeding the dissolution of LDHs [16].

Fig. 7c shows the distribution of Mg concentrations with column depth after those experiments. For 1 mM K^+ as background solution, the extracted concentrations of Mg in soil column and soil-LDHs column increased with depth. The difference of Mg concentrations (Fig. 7d, [Mg]) between soil and soil-LDHs is referred to the indication for the concentration of LDHs. The distribution of LDHs in the presence of 1 mM K^+ has shown the similar tendency (Fig. 7d). However, the distributions of Mg from soil and LDHs-soil in presence of 10 mM K^+ and Ca^{2+} are relatively homogenous with depth. Those results indicated that Mg from both soil and LDHs are transported to the deeper layer in presence of 1 mM K^+ while the transport of LDHs was more repressive with larger IS and in the presence of divalent Ca^{2+}. Natural soil mineral surfaces (e.g. clay minerals) show a stronger affinity for divalent than monovalent cations [47]. Our results suggested that cation bridging in presence of Ca^{2+} and higher IS increased the strength of adhesive interaction, such that the transport of LDHs in soil column are limited in presence of divalent cation and higher IS.

4. Conclusion

Findings in this study provide important insight on the roles of LDHs, solution IS, cation valance, and soil colloids on the transport, retention, and remobilization of P in soils. Experimental and modelling results indicate that the transport of P was reduced by the addition of LDHs and divalent cation due to the increased irreversible retention of P in soil. The increase of IS for K^+ from 1 to 100 mM resulted in increased P retention in LDHs-soil system due to more inner-sphere complexes and increased adhesive force. Significant amount of phosphate could be desorbed and transported from LDHs-soil by the reduction of IS in the presence of K^+. The Fe/Al oxides-facilitated transport of P is possible by the large perturbations in soil solution chemistry such as IS reduction and cation exchange that reduced the adhesive force. These results suggest the potential for the application of LDHs to reduce the transport of P in soil. The dissolution and transport of LDHs in soil could be impeded in presence of high cation valence and IS. However, there is still potential risk of P transport from LDHs-soil to nearby river system, especially during rainfall or irrigation events that alter the solution chemistry.

Acknowledgments

This study was financially supported by the Major Science and Technology Program for Water Pollution Control and Treatment, National Water Grant (No. 2017ZX07202002), Shenzhen Science and Innovation Commission (Nos. JSGG20170412145935322), and the Development and Reform Commission of Shenzhen Municipality (urban water recycling and environment safety program).

Conflicts of interest

None.

Appendix A. Supplementary data

Supplementary data to this article can be found online at https://doi.org/10.1016/j.cej.2019.05.083.

References

[1] C. Novillo, D. Guaya, A. Allen-Perkins Avendaño, C. Armijos, J.L. Cortina, I. Cota, Evaluation of phosphate removal capacity of Mg/Al layered double hydroxides from aqueous solutions, Fuel 138 (2014) 72–79.
[2] R.V. Smith, C. Jordan, J.A. Annett, A phosphorus budget for Northern Ireland: inputs to inland and coastal waters, J. Hydrol. 304 (1–4) (2005) 193–202.
[3] Brandt, M., Ejhed, H., Rapp, L., 2009. Nutrient loads to the Swedish marine environment in 2006-Sweden's report for HELCOM's fifth pollution load compilation (Report 5995). Swedish Environmental Protection Agency, Stockholm, Sweden.
[4] C.V. Luengo, M.A. Volpe, M.J. Avena, High sorption of phosphate on Mg-Al layered double hydroxides: kinetics and equilibrium, J. Environ. Chem. Eng. 5 (2017) 4656–4662.
[5] M. Dadwhal, M. Ostwal, P. Liu, M. Sahimi, T. Tsotsis, Adsorption of arsenic on conditioned layered double hydroxides: column experiments and modeling, Ind. Eng. Chem. Res. 48 (2009) 2076–2084.
[6] E. Klumpp, C. Contreras-Ortega, P. Klahre, F.J. Tino, S. Yapar, C. Portillo, S. Stegen, F. Queirolo, M.J. Schwuger, Sorption of 2,4-dichlorophenol on modified hydrotalcites, Colloids Surf. 230 (1-3) (2003) 111–116.
[7] M. Everaert, R. da Silva, F. Degryse, M. McLaughlin, E. Smolders, Limited dissolved phosphorus runoff losses from layered double hydroxide and struvite fertilizers in a rainfall simulation study, J. Environ. Qual. 47 (2018) 371–377.
[8] M. Everaert, R. Warrinnier, S. Baken, J. Gustafsson, D. De Vos, E. Smolders, Phosphate-exchanged Mg–Al layered double hydroxides: a new slow release phosphate fertilizer, ACS Sustain. Chem. Eng. 4 (2016) 4280–4287.
[9] M. Everaert, F. Degryse, M. McLaughlin, D. Vos, E. Smolders, Agronomic effectiveness of granulated and powdered P-exchanged Mg-Al LDH relative to struvite and MAP, J. Agric. Food Chem. 65 (2017) 6736–6744.
[10] L. Benício, V. Constantino, F. Pinto, L. Vergütz, J. Tronto, L. da Costa, Layered double hydroxides: new technology in phosphate fertilizers based on nanostructured materials, ACS Sustain. Chem. Eng. 5 (2017) 399–409.
[11] M. Bernardo, G. Guimaraes, V. Majaron, C. Ribeiro, Controlled release of phosphate from layered double hydroxide structures: dynamics in soil and application as smart fertilizer, ACS Sustain. Chem. Eng. 6 (2018) 5152–5161.
[12] L. Paulo, F. Benício, V. Constantino, F. Pinto, L. Vergütz, J. Tronto, L. Costa, Layered double hydroxides: new technology in phosphate fertilizers based on nanostructured materials, ACS Sustain. Chem. Eng. 5 (2016) 399–409.
[13] M. Elimelech, J. Greory, X. Jia, Particle Deposition and Aggregation: Measurement, Modelling and Simulation, Butterworth-Heinemann, 2013.
[14] J.N. Israelachvili, Intermolecular and Surface Forces, revised third ed., Academic press, 2011.
[15] K.C. Khilar, H.S. Fogler, Migrations of Fines in Porous Media, Springer Science & Business Media, 1998.
[16] S. Torkzaban, J. Wan, T.K. Tokunaga, S.A. Bradford, Impacts of bridging complexation on the transport of surface-modified nanoparticles in saturated sand, J. Contam. Hydrol. 136–137 (2012) 86–95.
[17] J. Yang, J.L. Bitter, B.A. Smith, D.H. Fairbrother, W.P. Hall, Transport of oxidized multi-walled carbon nanotubes through silica based porous media: influences of aquatic chemistry, surface chemistry, and natural organic matter, Environ. Sci. Technol. 47 (24) (2013) 14034–14043.
[18] Y. Liang, S. Bradford, J. Simunek, M. Heggen, H. Vereecken, E. Klumpp, Retention and remobilization of stabilized silver nanoparticles in an undisturbed loamy sand soil, Environ. Sci. Technol. 47 (2013) 12229–12237.
[19] M. Zhang, S. Bradford, J. Šimůnek, H. Vereecken, E. Klumpp, Role of cation valance and exchange on the retention and colloid-facilitated transport of functionalized multi-walled carbon nanotubes in a natural soil, Water Res. 109 (2017) 358–366.
[20] G.J. Bouyoucos, Hydrometer method improved for making particle size analysis of soils, Agron. J. 54 (1962) 464–465.
[21] J. Šimůnek, M.T.V. Genuchten, M. Šejna, Recent developments and applications of the hydrus computer software packages, Vadose Zone J. 15 (7) (2016) 1–25.
[22] J.F. Schijven, J. Simunek, Kinetic modeling of virus transport at the field scale, J. Contam. Hydrol. 55 (1–2) (2002) 113–135.
[23] S.A. Bradford, S.R. Yates, M. Bettahar, J. Šimůnek, Physical factors affecting the transport and fate of colloids in saturated porous media, Water Resour. Res. 38 (12) (2002) 63-1-63-12.
[24] R.S. Mansell, S.A. Bloom, W.C. Downs, A transport model with coupled ternary exchange and chemisorption retention for hydrazinium cations, J. Environ. Qual. 30 (2001) 1540–1548.
[25] D.W. Marquardt, An algorithm for least-squares estimation of nonlinear parameters, J. Soc. Ind. Appl. Math. 11 (1963) 431–441.
[26] Y. Gao, J. Wu, Z. Zhang, et al., Synthesis of polypropylene/Mg_3Al-X (X = CO_3^{2-}, NO_3^-, Cl^-, SO_4^{2-}) LDH nanocomposites using a solvent mixing method: thermal and melt rheological properties, J. Mater. Chem. A 1 (2013) 9928–9934.
[27] M. Berber, I. Hafez, K. Minagawa, T. Mori, A sustained controlled release formulation of soil nitrogen based on nitrate-layered double hydroxide nanoparticle material, J. Soil Sediments 14 (2014) 60–66.
[28] W. House, Geochemical cycling of phosphorus in rivers, Appl. Geochem. 24 (1) (2003) 120–128.
[29] P. Wu, A. Yin, M. Fan, J. Wu, X. Yang, H. Zhang, C. Gao, Phosphorus dynamics influenced by anthropogenic calcium in an urban stream flowing along an increasing urbanization gradient, Landsc. Urban Plan. 177 (2018) 1–9.
[30] A.Y. Grosberg, T. Nguyen, B. Shklovskii, Colloquium: the physics of charge inversion in chemical and biological systems, Rev. Mod. Phys. 74 (2) (2002) 329–345.
[31] M. Jensen, H. Hansen, S. Hansen, P. Jøgensen, J. Magid, N. Nielsen, Phosphate and tritium transport through undisturbed subsoil as affected by ionic strength, J. Environ. Qual. 27 (1998) 139–145.
[32] J.F. Schijven, S.M. Hassanizadeh, Removal of viruses by soil passage: overview of modeling, processes, and parameters, Crit. Rev. Environ. Sci. Technol. 30 (2000) 49–127.
[33] J. Antelo, M. Avena, S. Fiol, R. Lopez, F. Arce, Effects of pH and ionic strength on the adsorption of phosphate and arsenate at the goethite–water interface, J. Colloid Interface Sci. 285 (2005) 476–486.
[34] Y. Arai, D.L. Sparks, ATR-FTIR spectroscopic investigation on phosphate adsorption mechanisms at the ferrihydrite-water interface, J. Colloid Interface Science 241 (2001) 317–326.
[35] M. Mallet, K. Barthélémy, C. Ruby, A. Renard, S. Naille, Investigation of phosphate adsorption onto ferrihydrite by X-ray photoelectron spectroscopy, J. Colloid Interface Sci. 407 (2013) 95–101.
[36] R. Rahnemaie, T. Hiemstra, W. van Riemsdijk, Geometry, charge distribution, and surface speciation of phosphate on goethite, Langmuir 23 (2007) 3680–3689.
[37] Y. Arai, K.J.T. Livi, D.L. Sparks, Phosphate reactivity in long-term poultry litter-amended southern delaware sandy soils, Soil Sci. Soc. Am. J 69 (2005) 616–629.
[38] X. Jiang, R. Bol, S. Willbold, H. Vereecken, E. Klumpp, Speciation and distribution of P associated with Fe and Al oxides in aggregate-sized fraction of an arable soil, Biogeosciences 12 (2015) 6443–6452.
[39] M. Badreddine, M. Khaldi, A. Legrouri, A. Barroug, M. Chaouch, A. De Roy, J.P. Besse, Chloride-hydrogenophosphate ion exchange into the zinc-aluminum-chloride layered double hydroxide, Mater. Chem. Phys. 52 (1998) 235–239.
[40] Y. Seida, Y. Nakano, Removal of phosphate by layered double hydroxides containing iron, Water Res. 36 (2002) 1306–1312.
[41] A.V. Radha, P. Vishnu Kamath, C. Shivakumara, Mechanism of the anion exchange reactions of the layered double hydroxides (LDHs) of Ca and Mg with Al, Solid State Sci. 7 (2005) 1180–1187.
[42] A. Halajnia, S. Oustan, N. Najafi, A.R. Khataee, A. Lakzian, Effects of Mg-Al layered double hydroxide on nitrate leaching and nitrogen uptake by maize in a calcareous soil, Commun. Soil Sci. Plant Anal. 47 (9) (2016) 1162–1175.
[43] J.J. Bravo-Suárez, E.A. Páez-Mozo, S.T. Oyama, Review of the synthesis of layered double hydroxide: a thermodynamic approach, Química Nova 27 (2004) 601–614.
[44] L.O. Torres-Dorante, J. Lammel, H. Kuhlmann, T. Witzke, H.W. Olfs, Capacity, selectivity, and reversibility for nitrate exchange of a layered double-hydroxide (LDH) mineral in simulated soil solutions and in soil, J. Plant Nutr. Soil Sci. 171 (2008) 777–784.
[45] L.O. Torres-Dorante, J. Lammel, H. Kuhlmann, Use of a layered double hydroxide (LDH) to buffer nitrate in soil: long-term nitrate exchange properties under cropping and fallow conditions, Plant Soil 315 (2009) 257–272.
[46] J.D. Willey, The effect of ionic strength on the solubility of an electrolyte, J. Chem. Educ. 81 (2004) 1644.
[47] S.B. Roy, D.A. Dzombak, Colloid release and transport processes in natural and model porous media, Colloids Surf. A 107 (1996) 245–262.